Desalination and Water Treatment
www.deswater.com

doi: 10.5004/dwt.2022.28159

250 (2022) 126–135
February

Continuous removal of cadmium and lead ions by biochar derived from date seeds in a packed column reactor

Krishnan Saravanakumar[a,*], Manickam Sathyamoorthy[b], Donipathi Mogili Reddy Prasad[c], Ramalingham Senthilkumar[a], Balakrishna Sankari Naveen Prasad[d]

[a]*Department of Engineering, University of Technology and Applied Sciences, Suhar, Sultanate of Oman, email: drsara.soh@cas.edu.om/krishsaravanaoman@gmail.com (K. Saravanakumar)*
[b]*Chemical Engineering, HCT-Ruwais Women's College, Ruwais, Abu Dhabi, UAE*
[c]*Petroleum and Chemical Engineering Programme Area, Faculty of Engineering, Universiti Teknologi Brunei, Gadong, Brunei Darussalam*
[d]*Department of Engineering, University of Technology and Applied Sciences, Salalah, Sultanate of Oman*

Received 24 September 2021; Accepted 6 January 2022

ABSTRACT

The ability of date seed-derived biochar (DSB) to remove cadmium(II) and lead(II) from single and multi-solute solutions in packed column have been investigated. These column trials were conducted to understand the effects of column parameters such as bed depths, initial Cd(II)/Pb(II) concentrations and flow rates. The results indicated that the metal uptake of DSB decreased with increase in flow rate, and decrease in initial metal concentration and bed depth values. At a flow rate of 0.3 L/h, bed height of 25 cm, and initial metal concentration of 1 mmol/L, DSB recorded maximum Cd(II) and Pb(II) uptake values of 0.525 and 0.462 mmol/g, respectively. The continuous adsorption data models such as Yoon–Nelson, Thomas, and modified dose-response equations were utilized. Multi-component column studies were also performed and the results indicated decreased uptake of Cd(II) and Pb(II) by DSB due to competition. At optimized conditions, DSB recorded 0.447 and 0.449 mmol/g for Cd(II) and Pb(II), respectively, in multi-solute system. The column elution and subsequent reuse of DSB for next cycle was possible with 0.01 M HCl as elutant. The column regeneration was attempted for three cycles and the results indicated that DSB produced consistently high Cd(II) and Pb(II) removal efficiencies and uptakes.

Keywords: Wastewater treatment; Biochar; Date seed; Multi-component systems; Water quality

1. Introduction

Due to increased urbanization and industrialization, heavy metal pollution is a major environmental problem. Industries such as iron and steel, battery manufacture, metallurgy, electroplating, electrolysis, mining, tanneries, petroleum refining and pesticides release heavy metals into discharge waters [1–3]. Heavy metals are non-degradable as well as persistent substances that accumulate in human body through food chain thereby cause risk to human health [4,5]. Lead and cadmium are important heavy metals often employed in many industries and thus present in industrial discharge. In particular, lead has been widely used in the manufacture of storage batteries, automobiles, smelting, and electroplating [6]. Effluent waters discharged from these industries are generally comprised of high lead concentration. Currently, the discharge limit for lead is set at 0.1 mg/L according to National Environmental Agency, Singapore [7]. Lead is very toxic to living beings and lead poisoning in humans affects the nervous system

* Corresponding author.

and gastrointestinal track [8,9]. On the other hand, cadmium also poses severe hazard owing to its severe risks in humans including bone lesions, renal disturbances and cancer [6]. Thus, there is a definite need to develop cheap and efficient techniques for the treatment of Cd and Pb-bearing industrial effluents.

For removal of metals from industrial effluents, several conventional techniques were proposed and practiced, which includes ion-exchange, reverse osmosis, membrane filtration, activated carbon adsorption and biosorption [10–13]. However, most of these techniques present practical problems including high cost and energy requirement, high chemical usage, poor effectiveness and less selectivity [14]. Owing to these demerits, the research community is still looking for a cheap, environmentally benign, and practical technique for metal removal.

Our previous study has highlighted that date seed-derived biochar as an effective adsorbent for sequestration of Cd and Pb-bearing wastewaters in batch mode of operation [15]. However, it should be emphasized that batch experimental results offer only preliminary information regarding the sorption performance of material. These batch data may not be useful for industrial/large operations where residence time may not be adequate to achieve equilibrium [16]. Therefore, to gather evidence for applicability of the date-seed derived biochar in real applications, it is very important to further conduct continuous flow experiments. Several researchers have pointed out that continuous flow adsorption experiments can be effectively conducted using packed bed column as it offers practical use of concentration gradient as the driving force for adsorption [17–19]. In addition, the packed column is economically feasible and simple in operation, and could be scale-up easily to real wastewater schemes with good accuracy [20].

In addition, most industrial effluents contain multiple metal ions and exhibit complexity. However, very few research focused on multi-solute adsorption systems [21]. Several factors limit the multi-solute adsorption studies, the important being the assessment of competition between metal ions during sorption onto functional groups on the adsorbent surface [22]. During column operation, multi-solute solutions may cause uneven concentration gradient due to solute competition thereby overshooting specific metal ions. This is seldom studied; however, very important to translate laboratory studies to real applications. Therefore, the present study employed date seed-derived biochar (DSB)-loaded packed column for the sorption of Cd and Pb from single and multi-component systems.

2. Materials and methods

2.1. Biochar preparation and chemicals

Phoenix dactylifera (date fruit) was procured locally and the seeds were removed manually. The seeds were subsequently rinsed with deionized water. The washed seeds were then dried in an oven at 100°C for 12 h. After drying, the samples were grounded using ball mill to desired sizes. For pyrolysis, about 100 g of dried grounded date seeds was kept in a crucible covered with aluminium foil with two small holes. The crucible then placed in an electrical muffle furnace which was initially supplied with N_2 to facilitate low-O_2 environment. The muffle furnace was heated to 350°C and maintained at the same condition for 2 h [23]. Once the pyrolysis process was completed after 2 h, the furnace was allowed to cool down to room temperature. The biochar formed was then stored in a desiccator and used for adsorption trials.

The stock Cd and Pb solutions were prepared using cadmium nitrate tetrahydrate and lead nitrate salts, respectively. All chemicals were of analytical grade and were procured from Sigma-Aldrich.

2.2. Column experiments

Continuous-flow adsorption experimental trials were performed using a 35 cm (height) and 2 cm (ID) glass column. The column was attached with an adjustable plunger with a 0.5 mm stainless sieve at the top. On the other hand, glass wool was placed along with a 0.5 mm stainless sieve at the bottom. To maintain uniform solution flow inside the column, glass beads (1.5 mm in diameter) was placed at column base up to height of 2 cm.

The column was initially loaded with required quantity of DSB to achieve preferred bed height. After sorbent loading, a known initial metal concentration solution was pumped upward using a peristaltic pump at the required flow rate. Once the solution flow through the column, the samples coming from the exit (column top) were collected at different time periods and subsequently measured for Cd or Pb ions. Once the exit metal concentration reached 0.97 times of the initial concentration, the column was assumed to be exhausted and operation was ceased. The column experimental conditions were optimized by changing flow rate (0.3–0.6 L/h), bed height (15–25 cm) and initial metal concentration (0.5–1.0 mmol/L).

Once the column exhausted, the Cd/Pb-loaded DSB was rejuvenated using 0.01 M hydrochloric acid. The desorbent flow rate was maintained at 0.6 L/h and the sample exiting the column was analyzed using inductively coupled plasma-optical emission spectroscopy at different time periods. Once the column was completely eluted, the DSB column bed was washed using DI water until the pH of the exit solution was stabilized near 7.0. After washing, the column was operated again by feeding fresh solutions and these cycles of adsorption and desorption were repeated thrice to assess DSB adsorption potential.

2.3. Analyses of column results

The breakthrough curve was plotted with column operational time on the x-axis and outlet Cd/Pb concentration on the y-axis. The total quantity of metal ions adsorbed by DSB (m_{ad}) was determined by multiplying the area above the breakthrough curve with the influent flow rate (F). The metal uptake by the DSB column bed (Q_{col}) was estimated by dividing m_{ad} by amount of DSB loaded inside column.

The other column parameters were determined through following equations [16]:

Volume of the treated wastewater:

$$V_{eff} = F \cdot t_e \quad (1)$$

Total quantity of metal sent to column:

$$m_{\text{total}} = \frac{C_0 \cdot F \cdot t_e}{1{,}000} \tag{2}$$

Total metal removal (%):

$$\text{Removal}\left(\%\right) = \frac{m_{\text{ad}}}{m_{\text{total}}} \times 100 \tag{3}$$

where C_0 (mmol/L) is initial Cd/Pb concentration and t_e (h) is exhaustion time.

The total amount of metal desorbed (m_d) can be quantified by multiplying the area below the elution curve (time vs. outlet Cd/Pb concentrations) with the flow rate. Thus, the elution efficiency can be estimated using:

$$E\left(\%\right) = \frac{m_d}{m_{\text{ad}}} \times 100 \tag{4}$$

To describe column adsorption data obtained at different column parameters, several non-linear column model equations were utilized as below:

Thomas model [24]:

$$\frac{C_0}{C} = 1 + \exp\left(\frac{k_{\text{TH}}}{F}\left(Q_0 M - C_0 V_{\text{eff}}\right)\right) \tag{5}$$

Yoon–Nelson model [25]:

$$\frac{C}{C_0} = \frac{\exp\left(k_{\text{YN}} t - \tau k_{\text{YN}}\right)}{1 + \exp\left(k_{\text{YN}} t - \tau k_{\text{YN}}\right)} \tag{6}$$

Modified dose-response model [26]:

$$\frac{C}{C_0} = 1 - \frac{1}{1 + \left(V_{\text{eff}} / b_{\text{mdr}}\right)^{a_{\text{mdr}}}} \tag{7}$$

where Q_0 (mmol/g) is the maximum adsorption potential of DSB; k_{TH} (L/mmol h) is the Thomas model rate constant; V_{eff} (L) is the volume of metal solution supplied to column; t (min) is the Yoon–Nelson constant, which is used to quantify the time required to reach 50% adsorbate breakthrough; k_{YN} (1/min) is the Yoon–Nelson model rate constant; a_{mdr} and b_{mdr} are the modified dose-response model constants. The model equations were solved through non-linear regression using SigmaPlot software.

3. Results and discussion

3.1. Impact of bed depth on metal adsorption

Bed depth is a crucial column parameter that affects the adsorption performance of material towards the solute [27]. In the present study, the DSB bed depth was varied inside the column from 15 to 25 cm, whereas the flow rate and initial metal concentrations were kept constant at 0.3 L/h flow rate and 1 mmol/L, respectively. Fig. 1 shows the column sorption curves at different bed depths during removal of Cd and Pb by DSB. The results confirmed that DSB sorption performance improved with increase in bed depths. This is owing to existence of relatively high binding sites at higher bed depths. Also, as shown in Table 1, both breakthrough, exhaustion times as well as mass transfer zone surged with increase in bed depth. The presence of additional DSB at higher bed depths also improved the Cd and Pb sorptional uptakes. For instance, 0.432 mmol Cd/g and 0.396 mmol Pb/g observed at 15 cm bed height increased to 0.525 mmol Cd/g and 0.462 mmol Pb/g at 25 cm.

3.2. Influence of flow rate on metal adsorption

Flow rate is also a crucial factor as it decides the contact time of metal ions inside the column and therefore influences the potential of sorbent during industrial wastewater schemes [28]. In order to utilize complete adsorption potential of adsorbent, it is vital to determine optimum flow rate. In the present study, the flow rate was varied from 0.3 to 0.6 L/h, whereas the bed depth and initial metal concentrations were kept constant at 25 cm and 1 mmol/L, respectively. The breakthrough curves obtained for DSB bed at different flow rates during sorption of Cd and Pb are presented in Fig. 2. Upon increasing the flow rates, DSB exhibited sharp breakthrough curve and shortened mass transfer zone due to premature exhaustion and breakthrough times. The sorptional capacity of DSB got hindered due to elevated flow rates as 0.525, 0.445 and 0.349 mmol/g for Cd; and 0.462, 0.421 and 0.337 mmol/g for Pb were observed at 0.3, 0.45 and 0.6 L/h, respectively. The reason that minimal flow rate resulted in maximum adsorption capacity is that low flow rate gave adequate contact time for solute to interact with functional groups of DSB bed [16]. On comparing the results as presented in Table 1, 0.3 L/h was identified as an optimal flow rate for Cd and Pb by DSB bed.

3.3. Impact of initial solute concentration on metal sorption

Next, the influence of initial concentration of metal ions was studied as the concentration difference acts as a driving force for adsorption [29]. The initial Cd/Pb concentrations were varied from 0.5 to 1 mmol/L, whereas the bed depth and flow rate were kept constant at 25 cm and 0.3 L/h, respectively. Table 1 shows the findings of column parameters and Fig. 3 shows the breakthrough curves of Cd/Pb sorption by DSB. The minimal influent metal concentration resulted in extended breakthrough owing to the presence of excess binding sites compared to the magnitude of metals (minor concentration gradient). In general, lower initial concentration resulted in delayed breakthrough and exhaustion time, widened sorption zone, decreased metal uptake, and reduced % metal removal (Table 1). However, the column sorption potential of DSB enhanced with surge in initial metal concentrations. At inlet metal concentration of 0.5, 0.75 and 1 mmol/L, DSB produced metal Cd sorptional uptakes of 0.450, 0.452 and 0.525 mmol/g; and Pb uptake capacities of 0.420, 0.439 and 0.462 mmol/g, respectively.

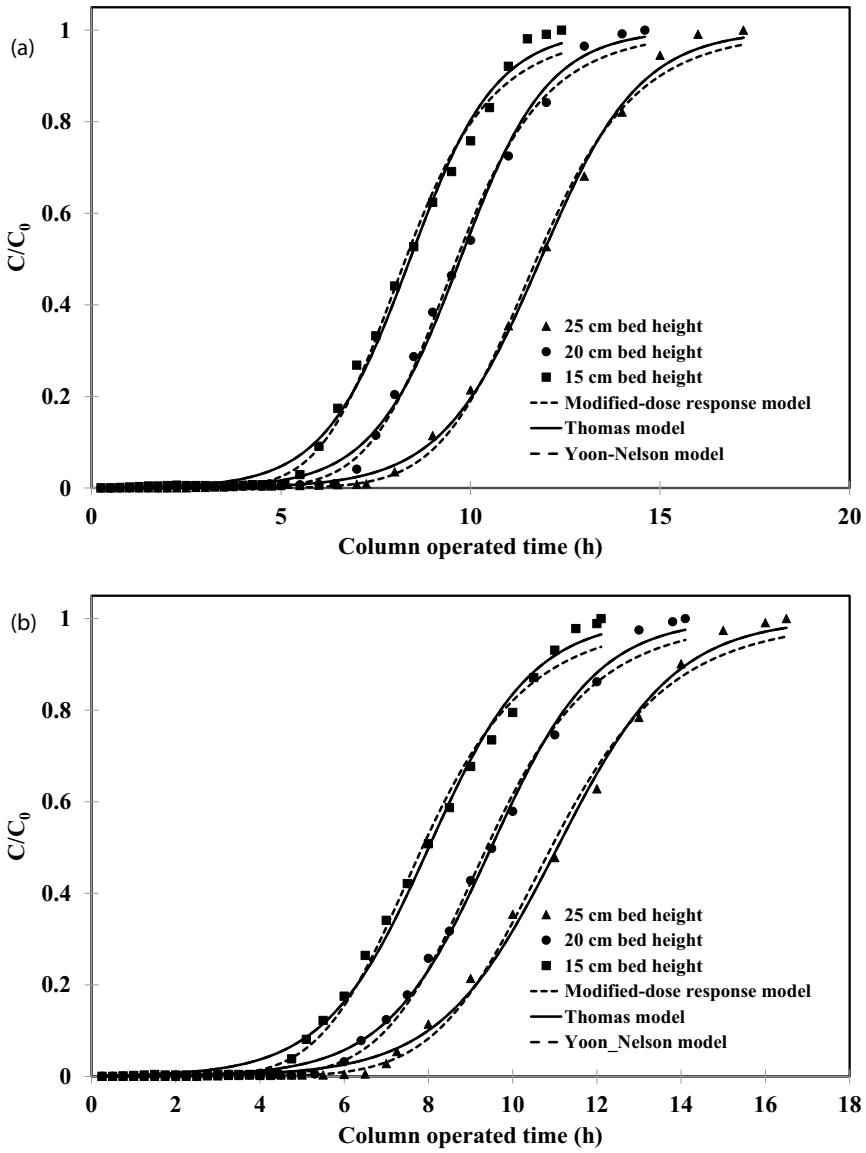

Fig. 1. Effects of bed height during column sorption of (a) Cd and (b) Pb by DSB.

3.4. Column data modeling

In order to successfully design and operate sorption column in large scale, it is important to predict the sorption breakthrough curves [30]. Several models were utilized to describe Cd/Pb-DSB column adsorption data, including the Thomas, Yoon–Nelson, and modified dose-response models [16,31]. The Thomas model is one of most widely used and effective adsorption model to describe continuous adsorption process. The model assumes the Langmuir adsorption–desorption kinetics and non-existence of axial dispersion [24]. As indicated in Figs. 1–3, the Thomas model provided good accuracy and representation of experimental Cd/Pb continuous data at all conditions examined. Table 2 illustrates the Thomas model constants (k_{TH} and Q_0) determined at various conditions. The Thomas model rate constant (k_{TH}) refers to the rate at which the metal ions are transported from solution to sorbent. As the initial metal concentrations and bed depth increases, the magnitude of k_{TH} reduced whereas increases with surge in flow rates. On the other hand, the maximum metal sorption capacity (Q_0) increased with increase in bed depths and initial metal concentrations whereas decreased with increase in flow rate. These opposite trends are as expected, as higher rate constants generally under exploit the full sorption capacity of DSB. The model produced very satisfactory predictions at all conditions examined (Table 2). The Yoon–Nelson model is formulated on the assumption that the rate of decline in the probability of sorption for each metal ion is proportional to the probability of metal ion adsorption and the probability of metal ion breakthrough on the adsorbent [32]. Figs. 1–3 show the Cd/Pb breakthrough curve prediction by the Yoon–Nelson model and the results (Table 2) also indicated that the model provided satisfactory predictions. Yan and Viraraghavan [26] developed a modified dose–response model, which reduces the error that results

Table 1
Continuous flow results during adsorption of Cd and Pb onto DSB

Bed depths (cm)	Initial metal concentrations (mmol/L)	Flow rates (L/h)	Volume of waste-water treated (L)		Total removal (%)		t_b (h)		t_e (h)		Δt (h)		Column uptake (mmol/g)	
			Cd	Pb	Cd	Pb	Cd	Pb	Cd	Pb	Cd	Pb	Cd	Pb
15	1.0	0.30	3.72	3.63	68.3	62.7	5.1	4.4	12.4	12.1	7.3	7.7	0.432	0.396
20	1.0	0.30	4.38	4.23	66.5	63.4	6.4	5.3	14.6	14.1	8.2	8.8	0.452	0.416
25	1.0	0.30	5.16	4.95	71.7	65.9	7.3	6.5	17.2	16.5	9.9	10	0.525	0.462
25	0.75	0.30	6.36	6.24	65.4	65.6	8.8	7.9	21.2	20.8	12.4	12.9	0.452	0.439
25	0.50	0.30	9.84	9.48	64.4	62.5	12.3	10.8	32.8	31.6	20.5	20.8	0.450	0.420
25	1.0	0.48	4.22	4.13	74.2	71.9	4.5	3.9	8.8	8.6	4.3	4.7	0.445	0.421
25	1.0	0.60	3.75	3.66	65.6	64.9	2.5	2.1	6.3	6.1	3.8	4	0.349	0.337

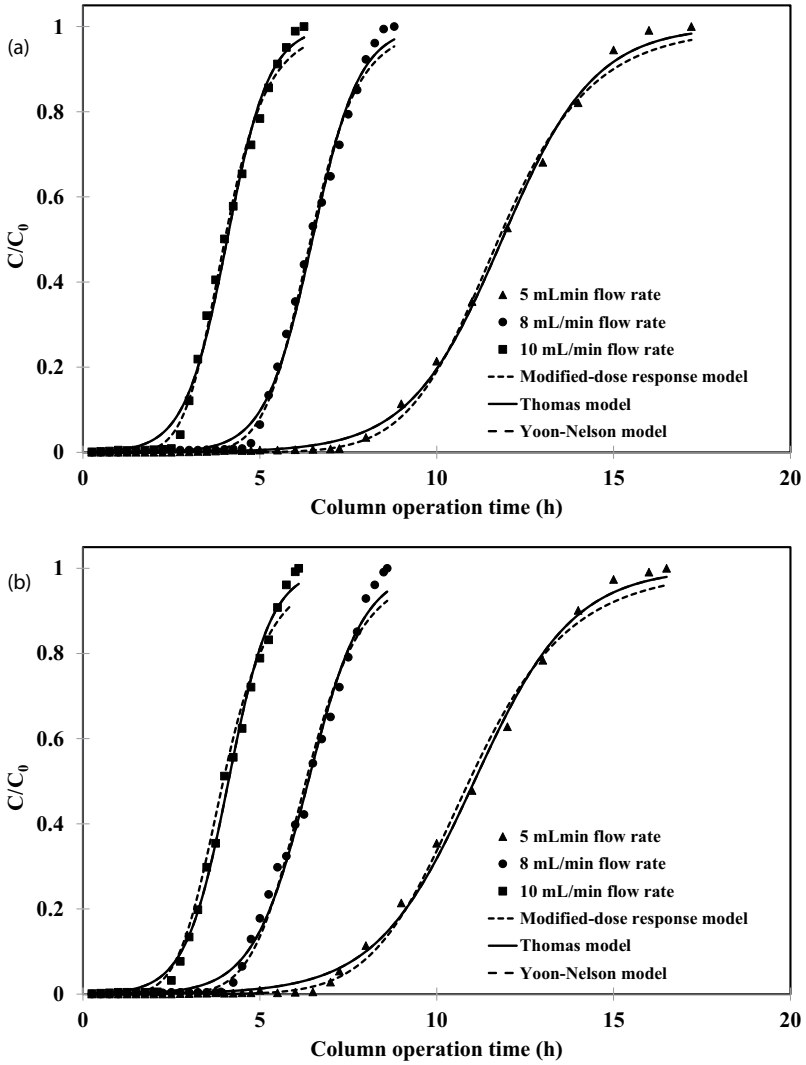

Fig. 2. Effects of flow rate during column sorption of (a) Cd and (b) Pb by DSB.

from use of the Thomas model, specifically during low or high time stages of breakthrough curve. Table 2 illustrates the modified dose-response constants (b_{mdr} and a_{mdr}) determined at various conditions. Figs. 1–3 show the Cd/Pb breakthrough curve prediction by the modified dose-response model and the results suggested that predictions were relatively good in line with the Thomas and Yoon–Nelson models.

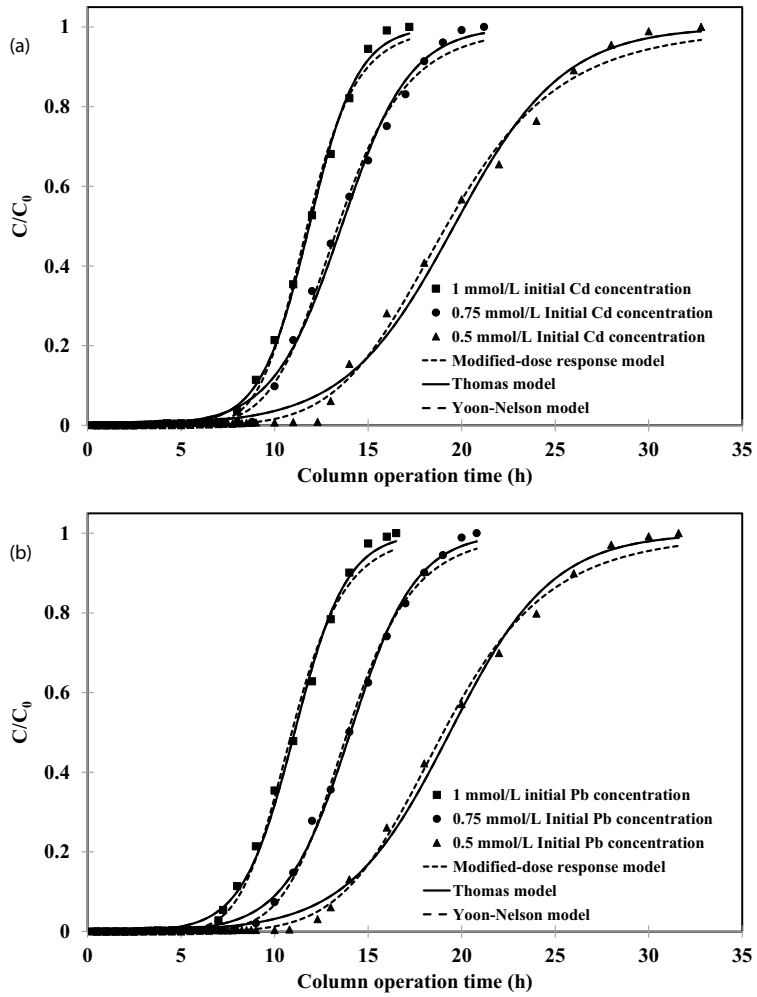

Fig. 3. Effects of initial concentration during column adsorption of (a) Cd and (b) Pb by DSB.

Table 2
Thomas, modified dose-response and Yoon–Nelson model parameters obtained for adsorption of Cd and Pb onto DSB

Metal	Bed depths (cm)	Initial concentrations (mmol/L)	Flow rates (L/h)	Thomas model				Modified dose-response model					Yoon–Nelson model			
				k_{TH}	Q_0	% error	R^2	a_{mdr}	b_{mdr}	Q_0	% error	R^2	k_{YN}	t	% error	R^2
Cd	15	1.0	0.30	0.880	0.429	0.245	0.994	7.26	2.49	0.423	0.238	0.995	0.881	8.40	0.251	0.996
	20	1.0	0.30	0.865	0.453	0.321	0.997	8.21	2.89	0.449	0.198	0.997	0.865	9.73	0.304	0.997
	25	1.0	0.30	0.764	0.504	0.145	0.999	8.99	3.52	0.500	0.545	0.998	0.764	11.85	0.135	0.999
	25	1.0	0.48	1.50	0.442	0.441	0.996	9.66	3.09	0.438	0.487	0.996	1.50	6.48	0468	0.996
	25	1.0	0.60	1.67	0.347	0.712	0.995	6.73	2.41	0.341	0.641	0.996	1.67	4.08	0.754	0.995
	25	0.75	0.30	0.728	0.433	0.387	0.997	7.27	4.02	0.427	0.294	0.998	0.546	13.6	0.364	0.997
	25	0.50	0.30	0.685	0.417	0.614	0.995	6.33	5.75	0.408	0.541	0.996	0.342	19.6	0.587	0.995
Pb	15	1.0	0.30	0.813	0.409	0.371	0.996	6.30	2.36	0.401	0.398	0.996	0.813	8.01	0.354	0.996
	20	1.0	0.30	0.801	0.442	0.224	0.998	7.42	2.82	0.437	0.289	0.997	0.801	9.49	0.221	0.998
	25	1.0	0.30	0.715	0.471	0.174	0.998	7.74	3.27	0.464	0.258	0.997	0.715	11.1	0.187	0.998
	25	1.0	0.48	1.28	0.434	0.487	0.994	8.02	3.02	0.429	0.852	0.992	1.28	6.37	0.448	0.994
	25	1.0	0.60	1.65	0.350	0.355	0.996	6.72	2.43	0.345	0.454	0.995	1.65	4.11	0.384	0.996
	25	0.75	0.30	0.762	0.449	0.085	0.999	7.95	4.17	0.444	0.198	0.998	0.571	14.1	0.097	0.999
	25	0.50	0.30	0.729	0.412	0.311	0.997	6.73	5.71	0.405	0.241	0.998	0.364	13.4	0.322	0.997

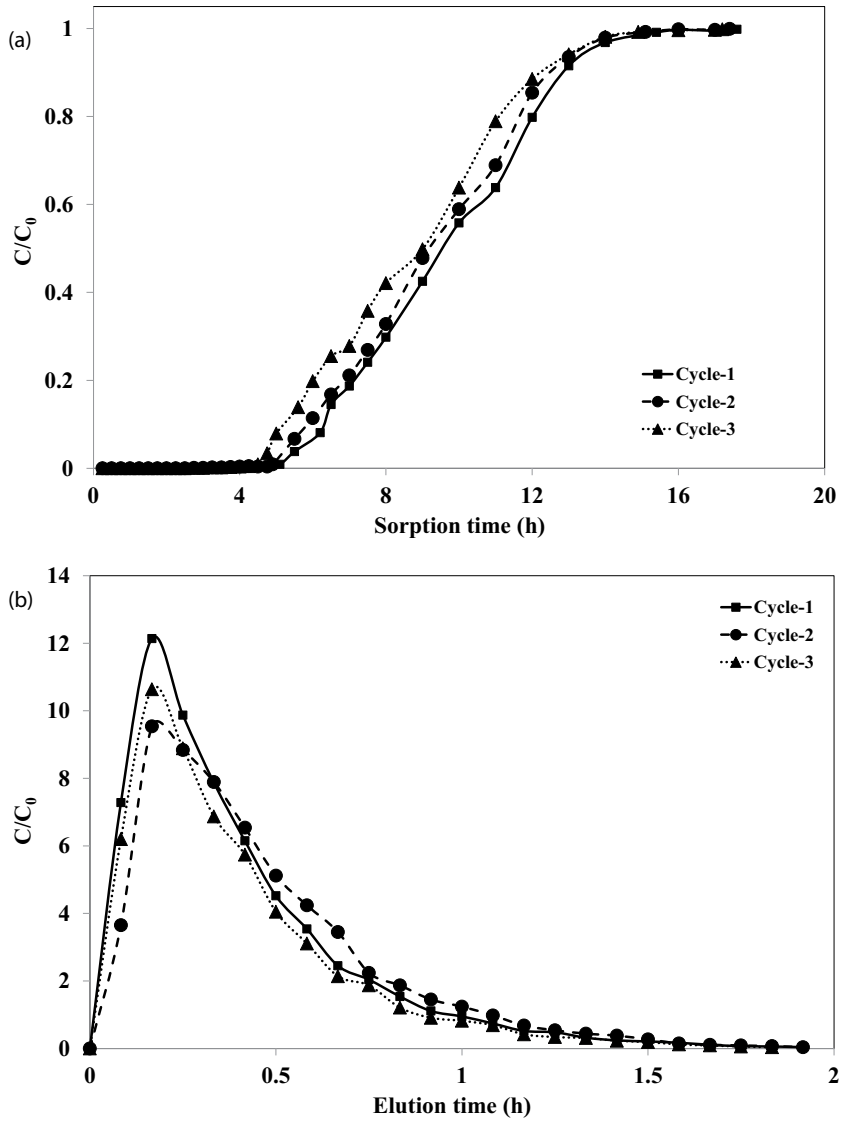

Fig. 4. Sorption and elution curves of Cd adsorption onto DSB during three cycles of adsorption–elution: (a) adsorption and (b) elution cycles.

3.5. Column multicomponent studies

As noted in previous sections, DSB exhibited single-component Cd and Pb sorptional capacities of 0.525 and 0.462 mmol/g, respectively. However, comparing the Cd and Pb ions on weight basis, DSB adsorbed more Pb (95.7 mg/g) than Cd (59.0 mg/g). The affinity of an adsorbent towards a particular metal ion can be correlated with its ionic radii and electronegativity. Of the two ions investigated, Pb exhibited better affinity towards DSB functional groups as the electronegativity of Pb (2.33) is more than that of Cd (1.69). Metal ions with higher ionic radius have smaller hydrated radius and lesser hydration energy. The metal ions with smaller hydrated radius sorbs effectively to the adsorbent compared to metal ions with larger radius [33]. Considering that Pb(II) possess larger ionic radius (119 pm), it would be expected to better bind the DSB surface compared to Cd(II) (109 pm). Similarly, electronegativity of Pb(II) (2.33) is higher than Cd(II) (1.69). Therefore, DSB favored Pb(II) compared to Cd(II) during sorption due to high ionic radius and electronegativity. Nevertheless, opposite trend was obtained when DSB sorptional uptake was considered in molar basis. This is basically due to higher atomic mass of Pb (207.2), compared to Cd (112.41).

When the influent contained both Cd and Pb ions (Figs. 4 and 5), DSB exhibited affinity towards Pb. It was evident that DSB sorption performance towards Pb was relatively unaltered as both single- and binary solute systems generated relatively similar breakthrough curves. This confirms that competition of Cd in binary solute system was minimal. In multi-solute system, the Pb breakthrough time was recorded as 6.2 h and the exhaustion time was 17.6 h. Whereas, Cd recorded a relatively premature breakthrough time of 5.1 h and exhaustion time of 15.4 h. This confirms that Pb negatively influences the sorption of Cd and preferentially occupies the functional groups of DSB. The Cd

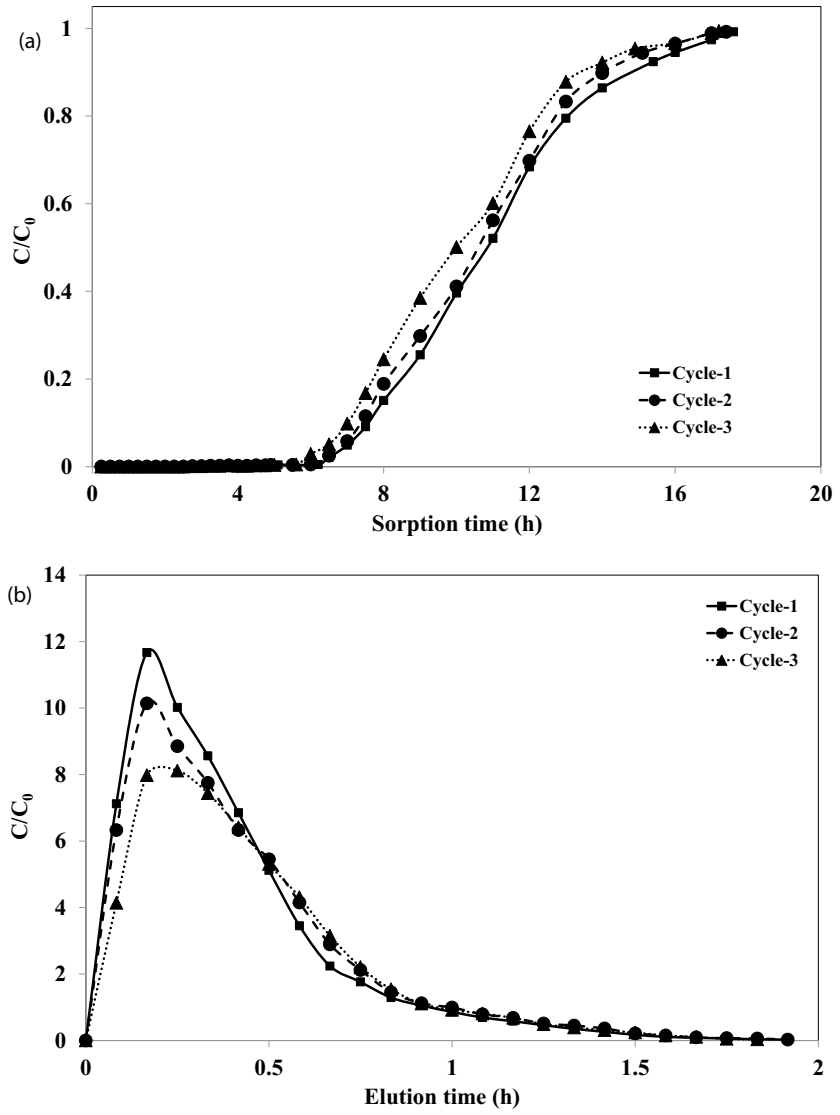

Fig. 5. Sorption and elution curves of Pb adsorption onto DSB during three cycles of adsorption–elution: (a) adsorption and (b) elution cycles.

and Pb column sorption capacities were recorded as 0.447 and 0.449 mmol/g, respectively.

3.6. Regeneration of DSB bed for sorption of Cd and Pb from multi-component solutions

The industrial adsorption-based wastewater treatment often requires adsorbent to be regenerated and reused for number of cycles to decrease process cost and dependability on the sorbent supply [34]. For the current study, DSB was desorbed and recycled for Cd/Pb adsorption for three adsorption–desorption cycles. The column was initially loaded with DSB to produce a bed depth and volume of and 25 cm and 78.5 mL, respectively. Table 3 shows the breakthrough and exhaustion times of Cd and Pb as well as metal sorptional uptake and % metal removal of three cycles examined. Figs. 4 and 5 show Cd and Pb breakthrough curves, respectively, obtained from three cycles. With the progress of each regeneration (sorption–desorption) cycle, breakthrough time decreased whereas exhaustion time surged, which caused widened mass transfer zone. These results clearly indicates that DSB deteriorated due to continuous use in repeated cycles. In addition, the DSB bed height decreased with the progression of regeneration cycles. However, the sorption capacity remained relatively constant in all cycles investigated (Table 3). These results clearly denote that change in column parameters during adsorption of Cd and Pb was not primarily due to physical damage of DSB, but owing to sorption binding sites, whose access to metal ions became tedious as the cycles progressed [35,36].

Desorption is important for overall accomplishment of sorbent recycle process. The desorbent should be efficient to remove all adsorbed solutes from the binding sites and non-damaging to DSB [37]. Figs. 4 and 5 display the Cd and Pb desorption curves, respectively, in all cycles investigated. The column desorption was performed at an average 1.9 h cycles

Table 3
Column parameters obtained during adsorption of Cd and Pb onto DSB in three adsorption–elution cycles

Cycle no.	Bed depths (cm)	Column uptake (mmol/g)		t_b (h)		t_e (h)		Δt (h)		dc/dt (mmol/L h)		Total metal removal (%)		Elution efficiency (%)	
		Cd	Pb	Cd	Pb	Cd	Pb	Cd	Pb	Cd	Pb	Cd	Pb	Cd	Pb
1	25.0	0.447	0.449	5.1	6.2	15.4	17.6	10.3	11.4	0.107	0.097	68.2	57.6	99.7	99.8
2	24.8	0.422	0.436	4.9	6.0	15.1	17.5	10.2	11.5	0.106	0.096	65.6	56.5	99.8	99.7
3	24.4	0.394	0.399	4.5	5.6	14.9	17.4	10.4	11.8	0.102	0.092	62.1	54.5	99.7	99.5

and stopped once the outlet metal reaches 0.024 mmol Pb/L or 0.044 mmol Cd/L. The elution curves exhibited a general trend with a sharp increase in metal concentrations in the initial time periods followed by a sharp concentration decline and final stationary stage. During the initial elution stage, the exit metal concentrations were very high. For example, at t = 10 min in cycle 1, 12.14 mmol/L of Cd and 11.67 mmol/L of Pb were present in the exit solutions.

The elutant, 0.01 M HCl, provided metal elution efficiencies greater than 99.5%. During 3 cycles, total volume of the Cd/Pb solution (1 mmol Cd/L and 1 mmol Pb/L) remediated by DSB bed was 15.66 L and total 0.01 M HCl solution used during desorption was 3.39 L. This corresponds to a concentration factor of 4.60. At the end of third cycle, DSB exhibited a comparatively high metal uptakes of 0.394 and 0.399 mmol/g for Cd and Pb, respectively, thereby portraying the competence of DSB to persist under extreme conditions as well as providing good Cd and Pb uptakes.

4. Conclusions

Thus, the current research indicated that the DSB is a practical and efficient adsorbent for continuous remediation of Cd and Pb from single and multi-solute systems. The experimental data obtained from an up-flow packed column were used to evaluate the impact of flow rate, initial solute concentration and bed depth on Cd and Pb removal by DSB. The results confirmed that minimal flow rate favored sorption, while higher bed depth and initial solute concentration produced better column remediation efficiency. At 25 cm bed depth, 1 mmol/L initial solute concentration and 0.3 L/h flow rate, DSB-loaded column portrayed 0.525 and 0.462 mmol/g sorptional capacities for Cd and Pb, respectively. The examined column models (modified dose-response, Thomas, Yoon–Nelson) provided good description of the experimental Cd and Pb data. With the aid of 0.01 M HCl as desorbing medium, the desorption and subsequent reuse of DSB column was possible. Only a minimal decrease in sorption uptake was observed as the sorption–desorption cycles progressed. Nevertheless, the DSB shown capacity to maintain high Cd and Pb uptakes greater than 0.394 and 0.399 mmol/g, respectively, in all three cycles examined. Thus, the current study recommends DSB as an efficient and practical sorbent for Cd and Pb. Future research should focus on performance of DSB for real industrial effluents.

Conflict of interest

No conflict of interest to declare.

Data availability statement

Data available on request from the authors.

References

[1] P.B. Tchounwou, C.G. Yedjou, A.K. Patlolla, D.J. Sutton, Heavy metals toxicity and the environment, Experientia Supplementum, 101 (2012) 133–164.
[2] K. Vijayaraghavan, T. Ashokkumar, Plant-mediated biosynthesis of metallic nanoparticles: a review of literature, factors affecting synthesis, characterization techniques and applications, J. Environ. Chem. Eng., 5 (2017) 4866–4883.
[3] J.P. Vareda, A.J.M. Valente, L. Durães, Assessment of heavy metal pollution from anthropogenic activities and remediation strategies: a review, J. Environ. Manage., 246 (2019) 101–118.
[4] K. Vijayaraghavan, F.D. Raja, Design and development of green roof substrate to improve runoff water quality: plant growth experiments and adsorption, Water Res., 63 (2014) 94–101.
[5] A.T. Jan, M. Azam, K. Siddiqui, A. Ali, I. Choi, Q.M. Rizwanul Haq, Heavy metals and human health: mechanistic insight into toxicity and counter defense system of antioxidants, Int. J. Mol. Sci., 16 (2015) 29592–29630.
[6] M. Jaishankar, T. Tseten, N. Anbalagan, B.B. Mathew, K.N. Beeregowda, Toxicity, mechanism and health effects of some heavy metals, Interdiscip. Toxicol., 7 (2014) 60–72.
[7] NEA, National Environmental Agency, Environmental Protection and Management (Trade Effluent) Regulations, Environmental Protection and Management Act, Chapter 94A, Section 77, 2008. Available at: https://sso.agc.gov.sg/Act/EPMA1999 (accessed November 10, 2020).
[8] K. Vijayaraghavan, U.M. Joshi, Chicken eggshells remove Pb(II) ions from synthetic wastewater, Environ. Eng. Sci., 30 (2013) 67–73.
[9] Z.A. Haghighat, E. Ameri, Synthesis and characterization of nano magnetic wheat straw for lead adsorption, Desal. Water Treat., 57 (2016) 9813–9823.
[10] M. Sathishkumar, S. Pavagadhi, K. Vijayaraghavan, R. Balasubramanian, S.-L. Ong, Experimental studies on removal of microcystin-LR by peat, J. Hazard. Mater., 184 (2010) 417–424.
[11] K.C. Khulbe, T. Matsuura, Removal of heavy metals and pollutants by membrane adsorption techniques, Appl. Water Sci., 8 (2018) 19, doi: 10.1007/s13201-018-0661-6.
[12] H. Sohrabi, E. Ameri, Adsorption equilibrium, kinetics, and thermodynamics assessment of the removal of the reactive red 141 dye using sesame waste, Desal. Water Treat., 57 (2016) 18087–18098.
[13] E. Cheraghi, E. Ameri, A. Moheb, Adsorption of cadmium ions from aqueous solutions using sesame as a low-cost biosorbent: kinetics and equilibrium studies, Int. J. Environ. Sci. Technol., 12 (2015) 2579–2592.
[14] K. Vijayaraghavan, D. Harikishore Kumar Reddy, Y.-S. Yun, Improving the quality of runoff from green roofs through synergistic biosorption and phytoremediation techniques: a review, Sustainable Cities Soc., 46 (2019) 101381, doi: 10.1016/j.scs.2018.12.009.

[15] K. Saravanakumar, B.S. Naveen Prasad, R. Senthilkumar, D.M. Reddy Prasad, D. Venkatesan, Single and competitive sorption potential of date seed-derived biochar during removal of lead(II) and cadmium(II) ions, Environ. Prog. Sustainable Energy, 40 (2021) e13690, doi: 10.1002/ep.13690.
[16] K. Vijayaraghavan, Y.-S. Yun, Polysulfone-immobilized *Corynebacterium glutamicum*: a biosorbent for Reactive black 5 from aqueous solution in an up-flow packed column, Chem. Eng. J., 145 (2008) 44–49.
[17] K. Vijayaraghavan, U.M. Joshi, Can green roof act as a sink for contaminants? A methodological study to evaluate runoff quality from green roofs, Environ. Pollut., 194 (2014) 121–129.
[18] D. Kumar, L.K. Pandey, J.P. Gaur, Metal sorption by algal biomass: from batch to continuous system, Algal Res., 18 (2016) 95–109.
[19] F. Afshariani, A. Roosta, Experimental study and mathematical modeling of biosorption of methylene blue from aqueous solution in a packed bed of microalgae *Scenedesmus*, J. Cleaner Prod., 225 (2019) 133–142.
[20] R. Senthilkumar, D.M. Reddy Prasad, L. Govindarajan, K. Saravanakumar, B.S. Naveen Prasad, Green alga-mediated treatment process for removal of zinc from synthetic solution and industrial effluent, Environ. Technol., 40 (2019) 1262–1270.
[21] K. Vijayaraghavan, Y.-S. Yun, Competition of Reactive red 4, Reactive orange 16 and Basic blue 3 during biosorption of Reactive blue 4 by polysulfone-immobilized *Corynebacterium glutamicum*, J. Hazard. Mater., 153 (2008) 478–486.
[22] K. Vijayaraghavan, M. Sathishkumar, R. Balasubramanian, Interaction of rare earth elements with a brown marine alga in multi-component solutions, Desalination, 265 (2011) 54–59.
[23] R. Senthilkumar, D.M. Reddy Prasad, L. Govindarajan, K. Saravanakumar, B.S. Naveen Prasad, Improved sorption of Reactive black 5 by date seed-derived biochar: isotherm, kinetic, and thermodynamic studies, Sep. Sci. Technol., 54 (2019) 2351–2360.
[24] H.C. Thomas, Heterogeneous ion exchange in a flowing system, J. Am. Chem. Soc., 66 (1944) 1664–1666.
[25] Y.H. Yoon, J.H. Nelson, Application of gas adsorption kinetics. I. A theoretical model for respirator cartridge service life, Am. Ind. Hyg. Assoc. J., 45 (1984) 509–516.
[26] G. Yan, T. Viraraghavan, M. Chen, A new model for heavy metal removal in a biosorption column, Adsorpt. Sci. Technol., 19 (1999) 25–43.
[27] B.E. Pérez Mora, S.E. Bellú, M.F. Mangiameli, S.I. García, J.C. González, Optimization of continuous arsenic biosorption present in natural contaminated groundwater, J. Chem. Technol. Biotechnol., 94 (2019) 547–555.
[28] M. Basu, A.K. Guha, L. Ray, Adsorption of cadmium ions by cucumber peel in continuous mode, Int. J. Environ. Sci. Technol., 16 (2019) 237–248.
[29] T. Bhagavathi Pushpa, J. Vijayaraghavan, S.J. Sardhar Basha, V. Sekaran, K. Vijayaraghavan, J. Jegan, Investigation on removal of malachite green using EM based compost as adsorbent, Ecotoxicol. Environ. Saf., 118 (2015) 177–182.
[30] T.V.N. Padmesh, K. Vijayaraghavan, G. Sekaran, M. Velan, Application of two- and three-parameter isotherm models: biosorption of acid red 88 onto *Azolla microphylla*, Biorem. J., 10 (2006) 37–44.
[31] E. Cheraghi, E. Ameri, A. Moheb, Continuous biosorption of Cd(II) ions from aqueous solutions by sesame waste: thermodynamics and fixed-bed column studies, Desal. Water Treat., 57 (2016) 6936–6949.
[32] Z. Aksu, F. Gönen, Biosorption of phenol by immobilized activated sludge in a continuous packed bed: prediction of breakthrough curves, Process Biochem., 39 (2004) 599–613.
[33] K. Vijayaraghavan, S. Gupta, U.M. Joshi, Comparative assessment of Al(III) and Cd(II) biosorption onto *Turbinaria conoides* in single and binary systems, Water Air Soil Pollut., 223 (2012) 2923–2931.
[34] A. Ronda, M. Calero, G. Blázquez, A. Pérez, M.A. Martín-Lara, Optimization of the use of a biosorbent to remove heavy metals: regeneration and reuse of exhausted biosorbent, J. Taiwan Inst. Chem. Eng., 51 (2015) 109–118.
[35] B. Volesky, J. Weber, J.M. Park, Continuous-flow metal biosorption in a regenerable *Sargassum* column, Water Res., 37 (2003) 297–306.
[36] M. Sathishkumar, A. Mahadevan, K. Vijayaraghavan, S. Pavagadhi, R. Balasubramanian, Green recovery of gold through biosorption, biocrystallization, and pyro-crystallization, Ind. Eng. Chem. Res., 49 (2010) 7129–7135.
[37] S. Lata, P.K. Singh, S.R. Samadder, Regeneration of adsorbents and recovery of heavy metals: a review, Int. J. Environ. Sci. Technol., 12 (2015) 1461–1478.